Electronic Supplementary Information

Scalable synthesis of djurleite copper sulphide ($Cu_{1.94}S$) hexagonal nanoplates from a single precursor copper thiocyanate and their photothermalproperties

Donghwan Yoon [a], Haneul Jin [a], Suho Ryu [b], Suhyun Park [a], Hionsuck Baik [c], Seung Jae Oh [d], Seungjoo Haam [e], Chulmin Joo [b*], and Kwangyeol Lee [a*]

[a] Department of Chemistry and Research Institute for Natural Sciences, Korea University, Seoul 136-701 (Korea)

[b] School of Mechanical Engineering, Yonsei University, Seoul 120-749 (Korea)

[c] Korea Basic Science Institute (KBSI), Seoul 136-713 (Korea)

[d] Medical Convergence Research Institute, College of Medicine, Yonsei University, Seoul, (Korea)

[e] Department of Chemical and Biomolecular Engineering, College of Engineering, Yonsei University, Seoul 120-749 (Korea)

*Corresponding authors: kylee1@korea.ac.kr (K. Lee), cjoo@yonsei.ac.kr (C. Joo)

Material Characterizations

Transmission electron microscopy (TEM) and high-resolution TEM (HRTEM) were performed on a TECNAI G2 20 S-Twin operated at 200 kV and TECNAI G2 F30 operated at 300 kV. Elemental mapping and energy dispersive X-ray spectra (EDX) were obtained with a FEI Titan Cubed 60-300 with Chemi-STEM technology and a JEOL ARM200F Cs STEM. X-ray diffraction (XRD) patterns were collected with a Rigaku Ultima III diffractometer system using a graphite-monochromatized Cu-Kα radiation at 40 kV and 40 mA.

Experimental Section

Large scale synthesis of $Cu_{1.94}S$ nanocrystals.

In a large scale synthesis of $Cu_{1.94}S$ nanocrystals, a slurry of 12.163 g CuSCN (Aldrich 99%) in 200 mL oleylamine (Aldrich 70%) was prepared in a 500 mL round bottom flask. After placing the reaction mixture under vacuum at 100°C for 10 min, the reaction mixture was charge with 1 atm Ar gas. Then the flask was directly placed in a hot oil bath, which was preheated to 250°C. After placing the flask in a hot oil bath, the temperature was set to 240°C. After heating for 30 min, the reaction mixture was cooled down to room temperature, washed with toluene and methanol, followed by centrifugal separation.

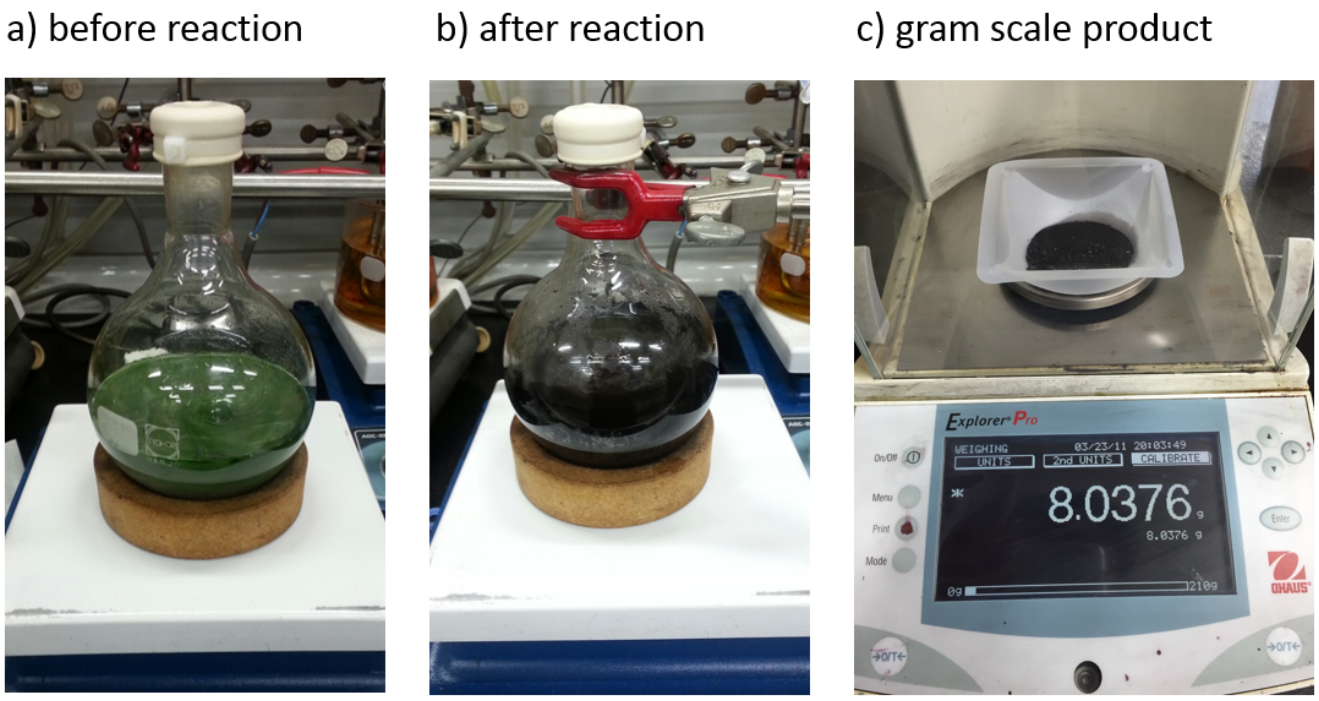

Fig. S1 Scalable synthesized nanocrystals powder. a) before reaction, b) after reaction, c) multi-gram scale product

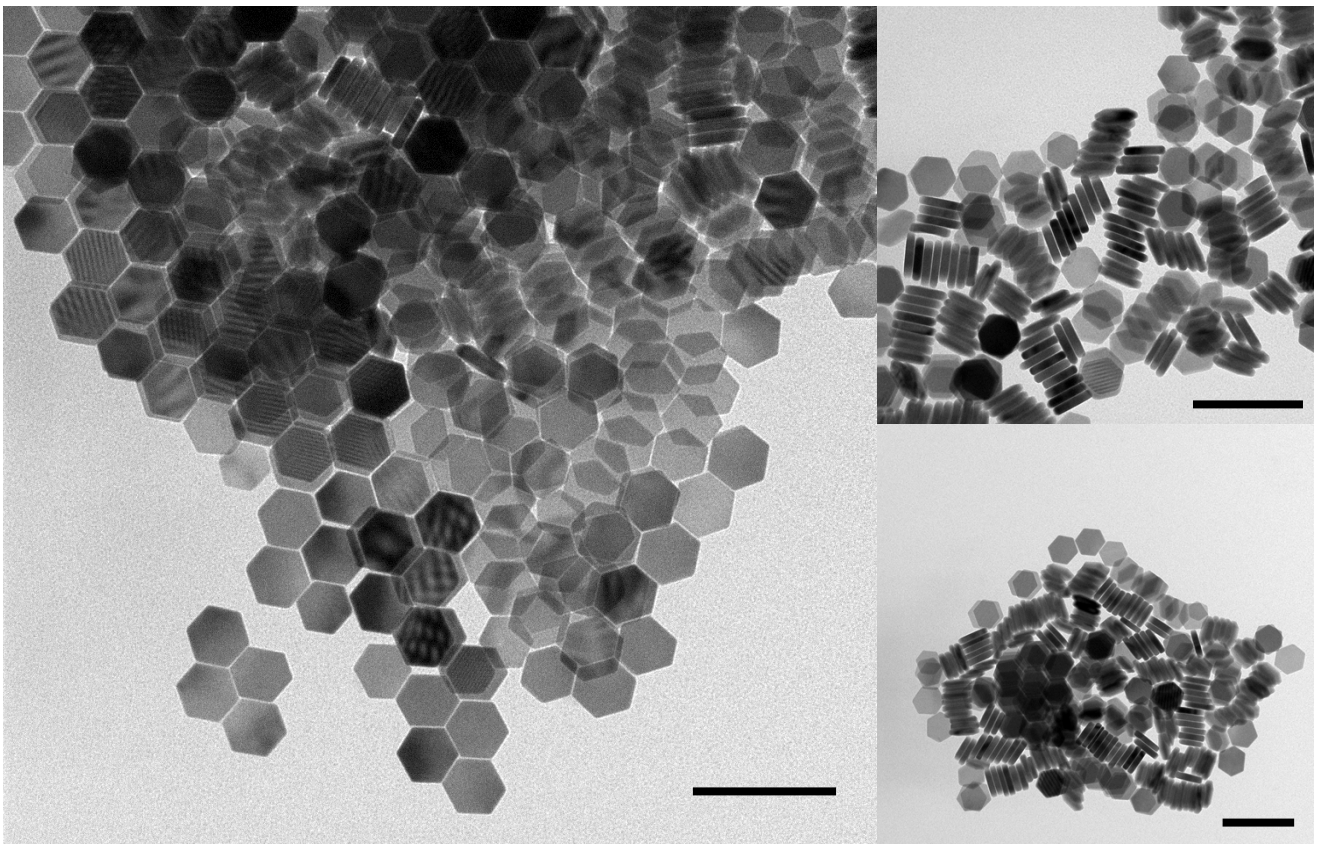

Fig. S2 TEM images of 88.1 ± 3.7 nm $Cu_{1.94}S$ nanocrystals. (scale bar = 200 nm)

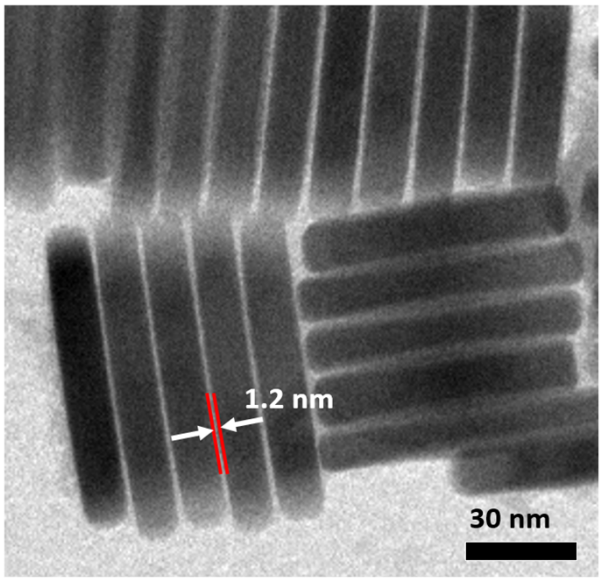

Fig. S3 TEM image of stacked 86.1 ± 2.9 $Cu_{1.94}S$ nanoplates. The distance between nanoplates is about 1. 28 nm corresponding to the thickness of interdigitated oleylamine bilayer.

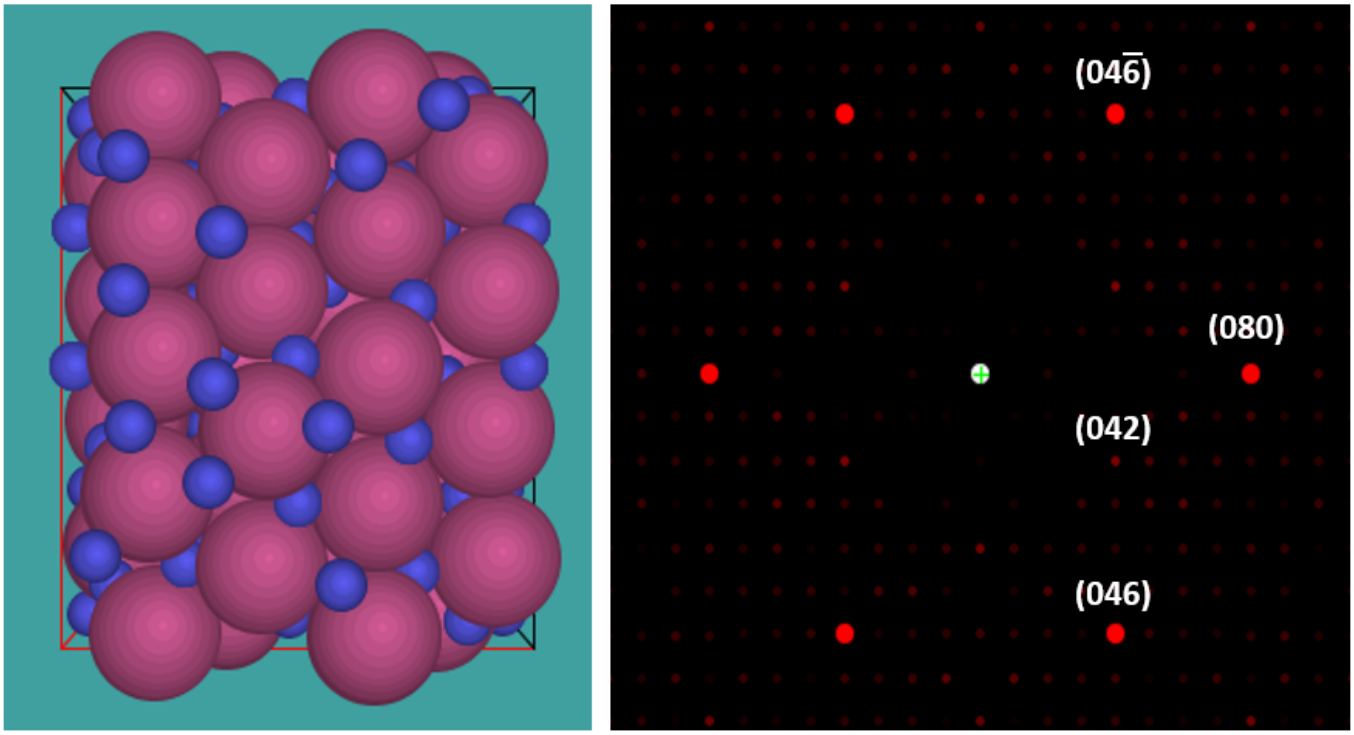

Fig. S4 Crystal structure analysis by JEMS (TEM diffraction and image simulation software) simulation. Atomic crystal structure in unit cell and FFT pattern with zone axis [-1, 0, 0] are shown. Red sphere – sulfur atom, blue sphere – copper atom

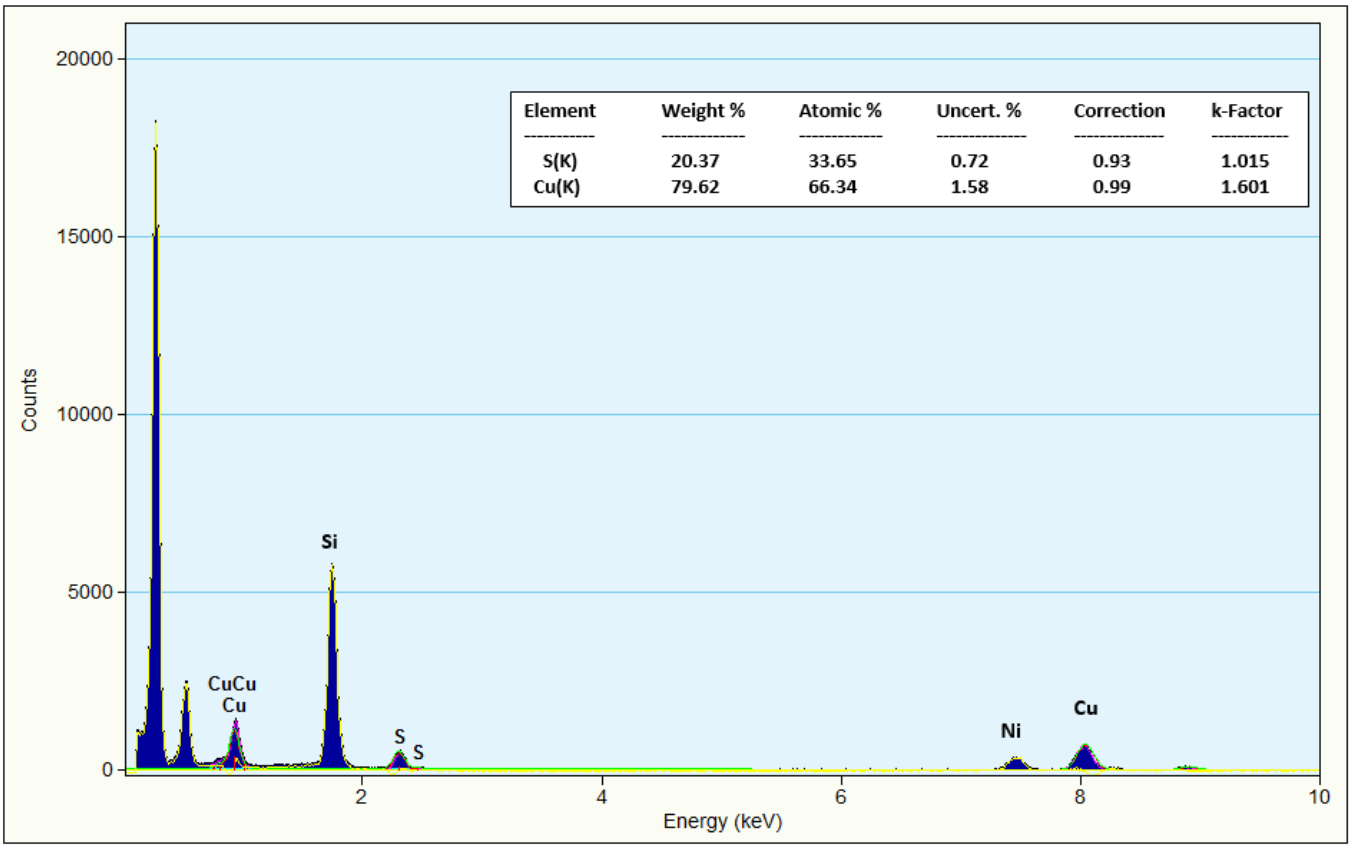

Fig. S5 Energy dispersive X-ray spectroscopy analysis of $Cu_{1.94}S$ nanocrystals prepared on a Ni grid.

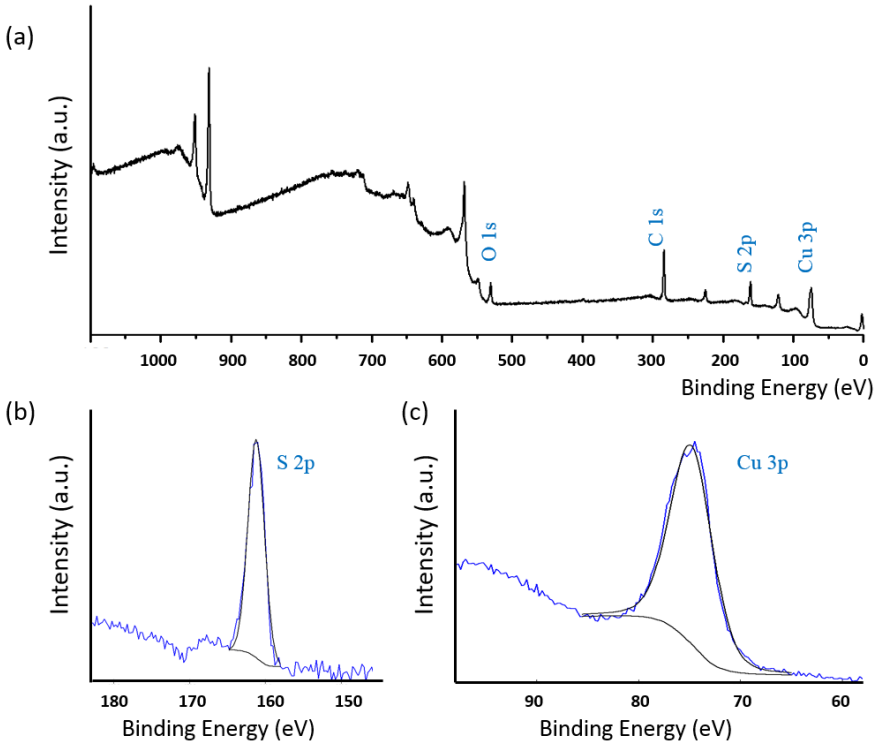

Fig. S6 X-ray Photoelectron Spectroscopy (XPS) spectra of $Cu_{1.94}S$ nanoplates.

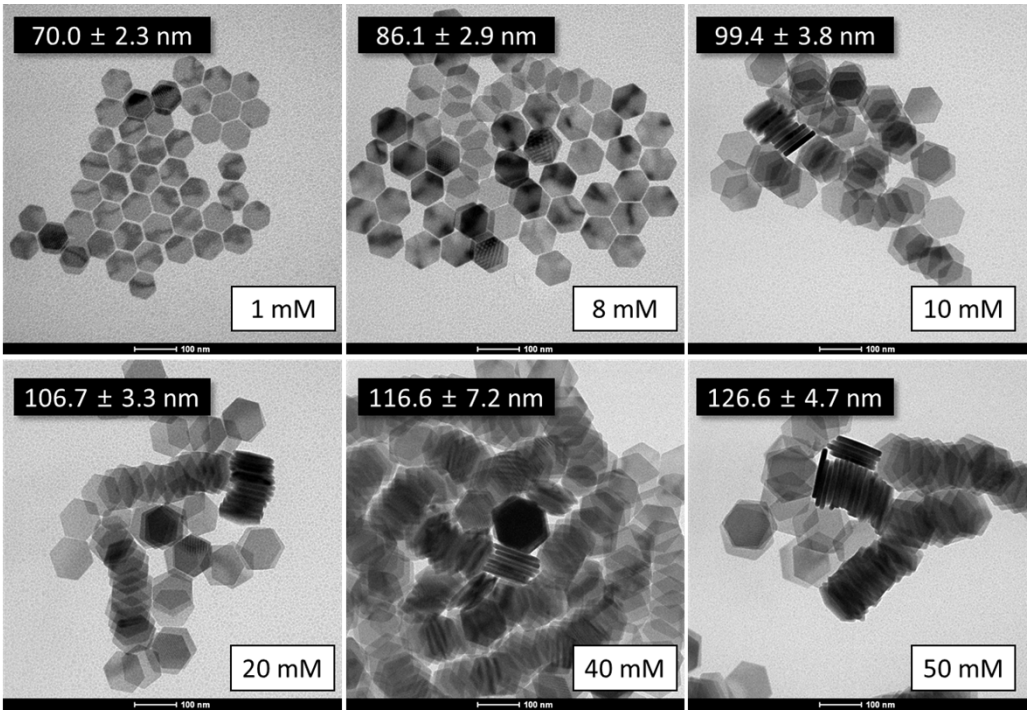

Fig. S7 TEM images of synthesized $Cu_{1.94}S$ nanocrystals at precursor concentrations shown.

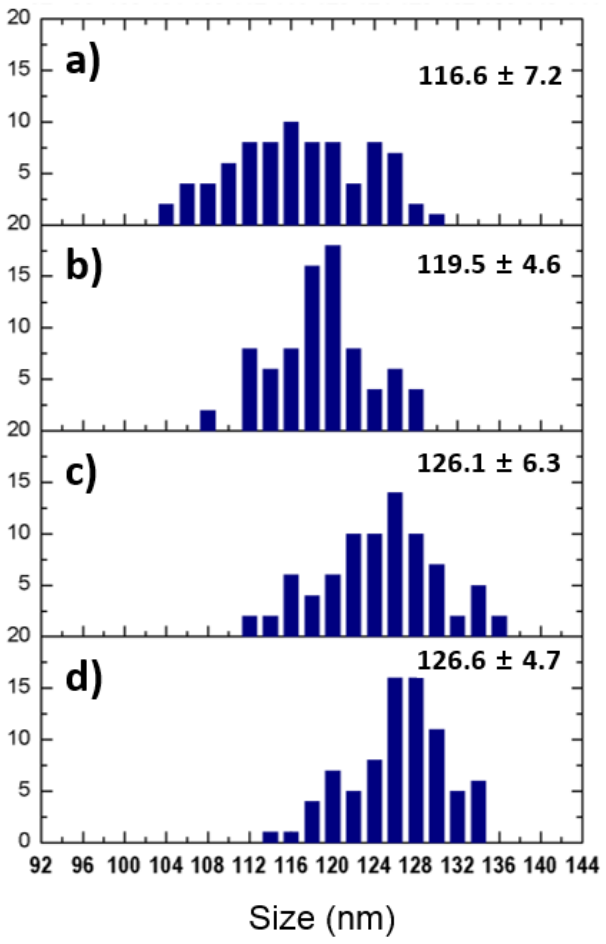

Fig. S8 The variation of size of $Cu_{1.94}S$ nanoplates by reaction time at 240°C. a) 5 min. b) 10 min. c) 20 min. d) 30 min.

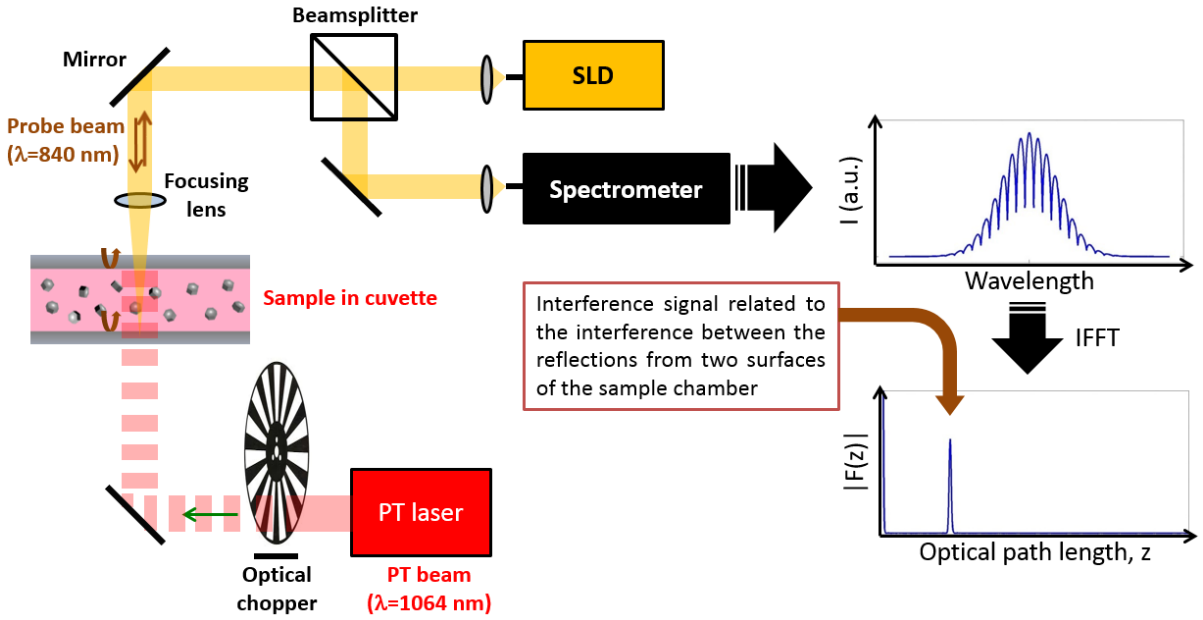

Fig. S9 Experimental configuration of PT OCR sensor. An 840 nm superluminescent laser diode was employed as the probe light source, and was directed to a cuvette containing the $Cu_{1.94}S$ nanoparticles. Upon its reflection from the cuvette, the light reflected from the top and bottom surfaces of inner chamber interferes with each other, producing interference fringe pattern in measured spectrum. By applying the inverse Fourier transform to the interference spectrum, path-length resolved complex-valued depth information could be obtained. In order to measure PT response of the nanoparticles, we illuminated the sample with a 1064 nm light during the measurement, since the $Cu_{1.94}S$ nanoparticles exhibit high absorption at ~1064 nm. The illumination direction of PT light was slightly tilted relative to the probe beam direction, so that it could not reach the spectrometer. We measure the phase changes of the interference signal of our interest upon the PT beam illumination. SLD: superluminescent laser diode.

Experimental setup and operation of our photothermal optical coherence reflectometer (PT OCR) can be found elsewhere. [1-3] In brief, it is based on a low-coherence spectral interferometer in which interference of reference and measurement light is spectrally measured, and converted into path-length resolved complex-valued information of a specimen. In the PT OCR setup (Fig. S8), an 840-nm probe light from a superluminescent laser diode illuminated the chamber filled with aqueous $Cu_{1.94}S$ nanoparticles. The 3-dB spectral bandwidth of the light source was ~50 nm. The reflections from the surfaces of the chamber were directed to the spectrometer (USB 4000, Ocean Optics, Inc., Canada). The spectrum related to the interference can be written as:

$$I(k) = 2\sum_{n} S(k)\sqrt{R_r R_s(z_n)}\cos\left(2kz_n\right),$$

where k is the wave number and $S(k)$ is the power spectral density of the light source. R_r and $R_s(z_n)$ are the reflectivities of the reference surface and nth measurement surface along the beam path, respectively, with the optical path-length difference between the two surfaces z_n. [1] In our case, the top surface of the inner chamber was used as a reference. Taking the inverse Fourier transform of the interference spectrum with respect to $2k$ produces a path-length resolved complex-valued information, $F(z)$. We locate the interference signal related to the interference between the reflections from the top and bottom surfaces of inner chamber, and monitor its phase as a function of time. The phase of the interference signal at the path-length z_n, $\phi(z_n)$, can be evaluated as:

$$\phi(z_n) = tan^{-1}\left[\frac{Im(F(z_n))}{Re(F(z_n))}\right].$$

Prior to 1064 nm PT laser illumination, no phase change is measured (Fig. S9a). Upon the PT laser illumination, the $Cu_{1.94}S$ nanoparticles absorb 1064 nm light energy and lead to a temperature increase due to the PT effect. Since the refractive index (n) varies as a function of temperature, the temperature alteration inside the chamber can be monitored by observing the phase change of the interference signal being measured (Fig. S9b). The measured phase change ($\Delta\phi$) is related to refractive index variation (Δn) as:

$$\Delta\phi = 2k_0 L\Delta n = 2\frac{2\pi}{\lambda_0}L\Delta n,$$

where k_0 and λ_0 are the center wave number and wavelength of the SD-OCR light, and L is the physical distance that the light passes through. In our case, L corresponds to the height of the inner chamber.

Measurement of phase changes due to PT effect can be performed either in continuous or intensity-modulated illumination of PT laser. In practice, however, external disturbances such as temperature drift and vibration may affect the reliable phase measurement. Therefore, we employed the intensity-modulation scheme, which enables highly sensitive measurement of phase changes with an improved signal-to-noise ratio (SNR) (Fig. S9c). By measuring the signal around the PT beam modulation frequency only, the measurement can be done more accurately as the effect of noise components at the other frequency ranges is minimized. The intensity-modulation was achieved by using an optical chopper (Optical chopper system with the chopper wheel, MC1F2, Thorlabs, USA) in the PT beam path. The acquired phase signal was Fourier transformed, and its magnitude centered at the modulation frequency, which we here denote PT OCR signal, was examined.

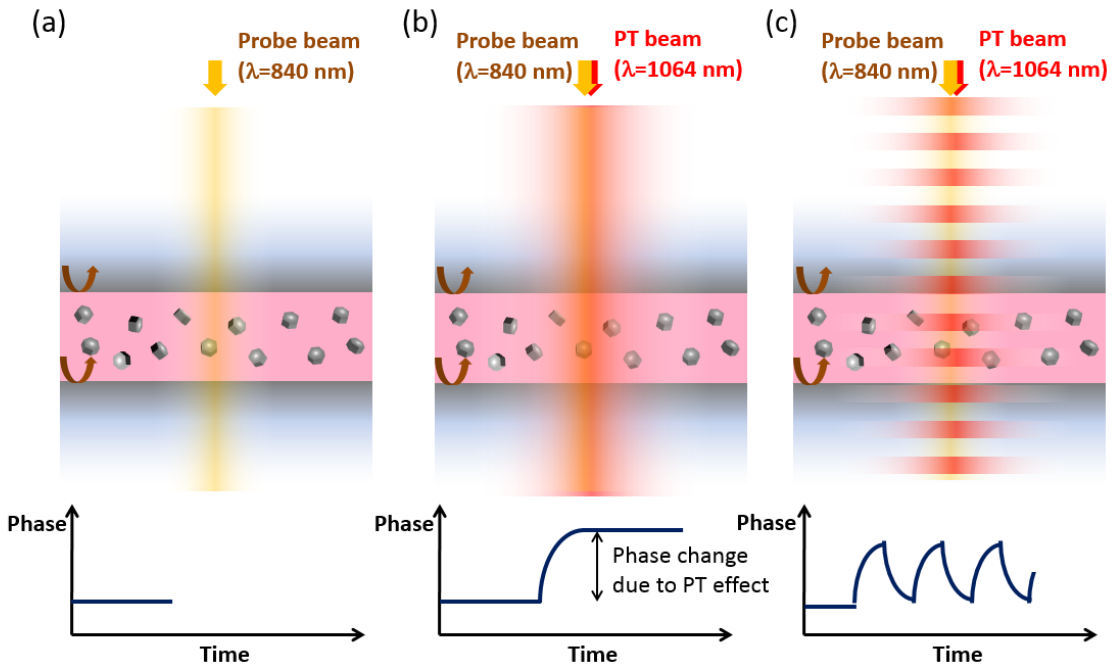

Fig. S10 The principle of PT effect detection using PT OCR. (a) The phase signal exhibits no notable change without excitation light. (b) The PT laser illumination induces temperature change inside PT light illumination volume, leading to change in SD-OCR phase signal. (c) The background noise such as temperature drift and mechanical vibration can be excluded by introducing the intensity modulation to PT light.

REFERENCE

1. C. Joo, T. Akkin, B. Cense, B. H. Park and J. F. de Boer, *Optics letters*, 2005, 30, 2131-2133.
2. C. Joo and J. F. de Boer, *Optics letters*, 2007, 32, 2426-2428.
3. J. Yim, H. Kim, S. Ryu, S. Song, H. O. Kim, K.-A. Hyun, H.-I. Jung and C. Joo, *Biosensors and Bioelectronics*, 2014, 57, 59-64.